JOURNAL OF MATERIALS SCIENCE 26 (1991) 1277–1286

Dynamic consolidation of rapidly solidified titanium alloy powders by explosives

H. L. COKER
Department of Materials and Metallurgical Engineering, New Mexico Institute of Mining and Technology, Socorro, New Mexico 87801, USA

M. A. MEYERS
Center of Excellence for Advanced Materials and Department of Applied Mechanics and Engineering Sciences, University of California, San Diego, La Jolla, California 92093, USA

J. F. WESSELS
General Electric Aircraft Engine Group, Cincinnati, Ohio 45215, USA

Consolidation of rapidly solidified titanium alloy powders employing explosively generated shock pressures was carried out successfully. The cylindrical explosive consolidation technique was utilized, and compacts with densities in the range 97 to 100% were produced. Better consolidation (with more interparticle melting regions and less cracking) was achieved by using a double tube design in which the outer tube (flyer tube) was explosively accelerated, impacting the powder container. Optical and transmission electron microscopy observations were carried out to establish microstructural properties of the products. It was observed that consolidation is achieved by interparticle melting occurring during the process. The interior of the particles in Ti-17 alloy exhibited planar arrays of dislocations and twin-like features characteristic of shock loading. Two dominant types of microstructures (lath and equiaxed) were observed both in Ti-662 and Ti-6242 + 1% Er compacts, and very fine erbia (Er_2O_3) particles were seen in the latter alloy. The micro-indentation hardness of the consolidated products was found to be higher than that of the as-received powder material; and the yield and ultimate tensile strengths were found to be approximately the same as in the as-cast and forged conditions. The ductilities (as measured by the total elongation) of the shock-compacted materials were much lower than those of the cast or forged alloys. Hot isostatic pressing of the shock-consolidated alloys increased their ductility. This enhancement in ductility is thought to be due to the closure of existing cracks. These excellent mechanical properties are a consequence of strong interparticle bonding between individual powder particles. It was also established that scaling up the powder compacts in size is possible and compacts with 50, 75, and 100 mm diameter were successfully produced.

1. Introduction

Shock consolidation of rapidly solidified metals is a process that has considerable potential. Consolidation can be achieved without prolonged exposure of the compact to high temperatures. The shock wave travelling through the powder promotes melting of the powder surface layers. This molten material is an effective bonding agent and is rapidly resolidified after the passage of the shock pulse.

Rapidly solidified materials therefore do not lose their unique microstructural characteristics during the shock consolidation stage. This technique is especially attractive for the new dispersion-strengthened titanium alloys currently under development. Rapid solidification is required to ensure a fine dispersion of a second phase (such as Er_2O_3) that is an effective strengthener of the alloy at high temperatures. There are, to the authors' knowledge, only a few reports of shock-consolidation of titanium alloy powders [1, 2]. Considerable work has been carried out on shock consolidation of rapidly solidified materials [3–9], but many roadblocks exist before this technology can be industrially implemented. The main problem is cracking of the compacts at both the microscopic and macroscopic levels. The three principal objectives of this investigation were (a) to demonstrate that rapidly solidified titanium alloy powders can be consolidated by shock waves, (b) to establish whether the process can be scaled up, and (c) to determine the mechanical properties and microstructural characteristics of the shock-consolidated alloys.

2. Materials and techniques

Three titanium alloys (REP Ti-17, PREP Ti-662, and RSR Ti-6242 + 1% Er) were used in this study. They were produced by three different but closely related techniques: rotating electrode process (REP), plasma rotating electrode process (PREP), and rapid solidification rate process (RSR). Ti-17 and Ti-662 powders

0022–2461/91 $03.00 + .12

TABLE I Nominal compositions of three titanium alloy powders

Material	Chemical composition (%)									
	Al	Sn	Zr	Mo	Cr	V	Tl	Cu	Er	Ti
Ti-17	5.0	2.0	2.0	4.0	4.0	–	–	–	–	bal.
Ti-662	6.0	2.0	–	–	–	6.0	1.0	1.0	–	bal.
Ti-6242	6.0	2.0	4.0	2.0	–	–	–	–	1.0	bal.

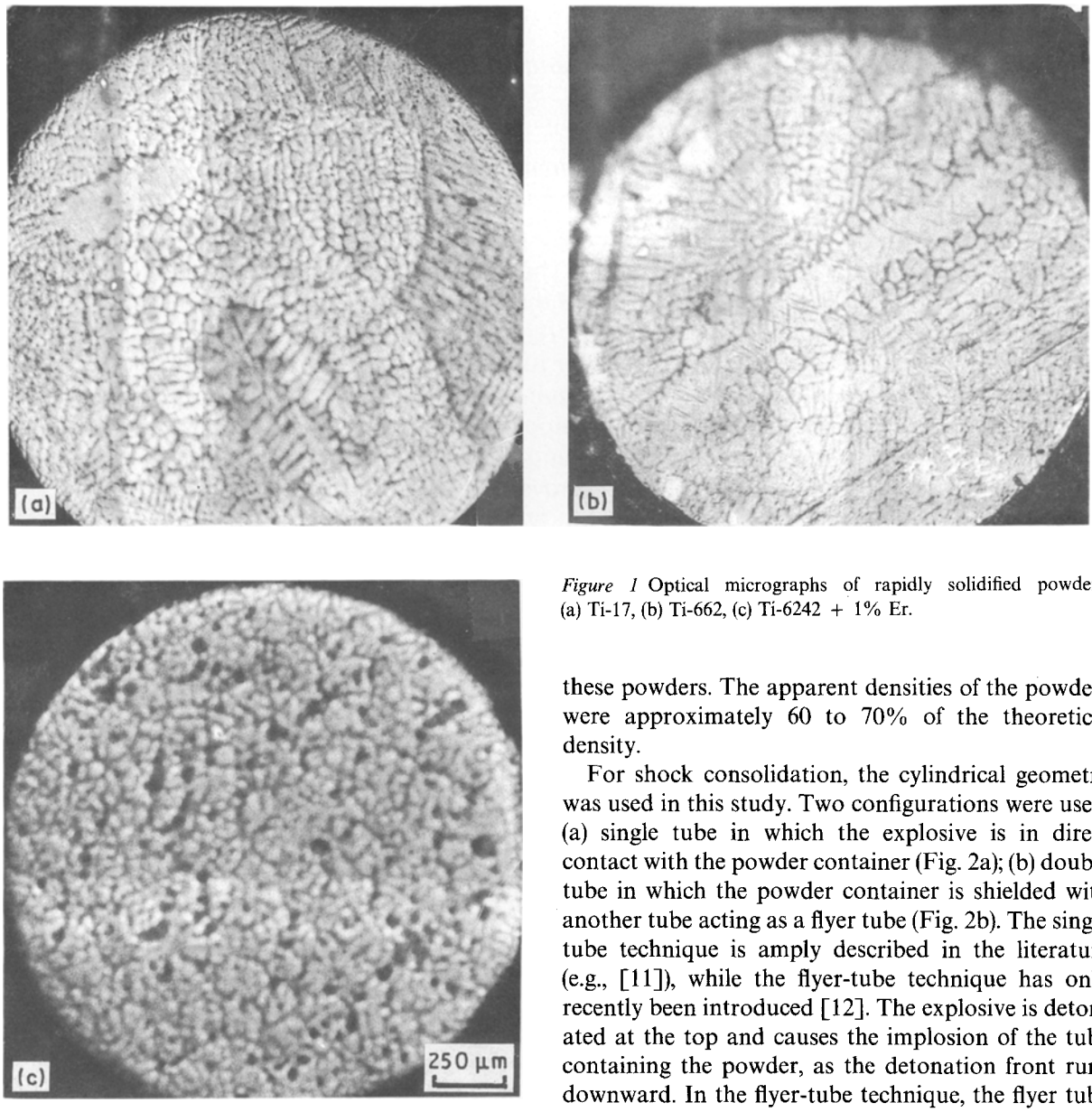

Figure 1 Optical micrographs of rapidly solidified powders. (a) Ti-17, (b) Ti-662, (c) Ti-6242 + 1% Er.

were produced by the Nuclear Metals Corporation, while Ti-6242 + 1% Er was produced by the Pratt and Whitney Aircraft Group of United Technologies. These titanium-based alloys were supplied by General Electric. Table I shows the nominal compositions of the three titanium alloys. The powder sizes ranged from 50 to 250 μm and they were spheroidal in shape. The Ti-6242 powder, prepared by the RSR technique, had a greater number of satellites than the other two powders. Fig. 1 shows the optical micrographs of cross-sections of the three powders. A microstructure varying between microcellular and microdendritic is seen in the three powders. These microstructures are consistent with the solidification rates encountered by these powders. The apparent densities of the powders were approximately 60 to 70% of the theoretical density.

For shock consolidation, the cylindrical geometry was used in this study. Two configurations were used: (a) single tube in which the explosive is in direct contact with the powder container (Fig. 2a); (b) double tube in which the powder container is shielded with another tube acting as a flyer tube (Fig. 2b). The single tube technique is amply described in the literature (e.g., [11]), while the flyer-tube technique has only recently been introduced [12]. The explosive is detonated at the top and causes the implosion of the tube containing the powder, as the detonation front runs downward. In the flyer-tube technique, the flyer tube impacts the powder tube, and the pressures generated are considerably higher than in the single-tube technique. A central mandrel was used along the cylinder axis to trap the Mach stem.

The initial pressure, as the shock wave enters the powder, can be calculated for the single- and double-tube geometries. The method is described in greater detail by Meyers and Wang [12]. The container tubes will be assumed to have a negligible thickness, in both configurations, in order to simplify the calculations. Fig. 3 shows the pressure–particle velocity curves for the fully dense Ti-17 alloy, for the Ti-17 powder at 67% of the theoretical density, for iron (flyer tube material) and for the explosives ANFO and TNT. The solid Hugoniot for Ti-17 was determined by a weighed

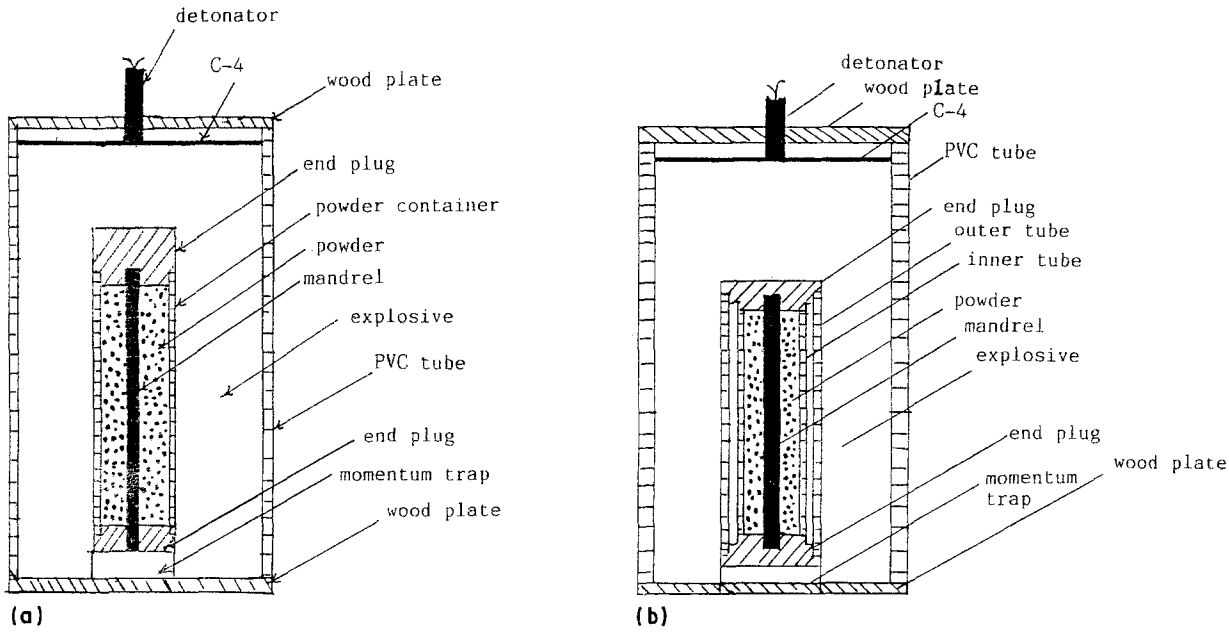

Figure 2 Systems used for shock consolidation of titanium alloys. (a) single tube, (b) double (or flyer) tube.

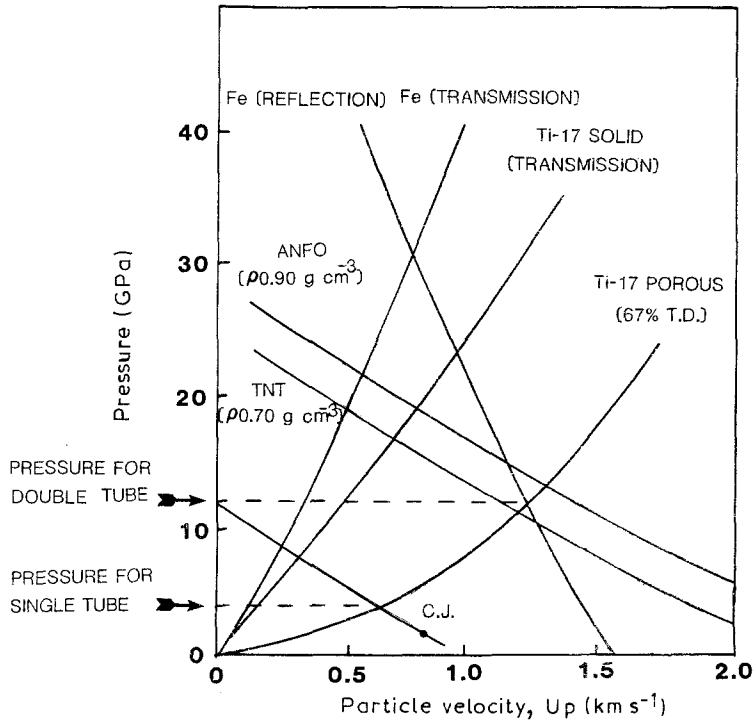

Figure 3 Pressure against particle velocity curves leading to determination of pressures for single-tube and flyer-tube techniques.

average from the equations-of-state of titanium, aluminium, molybdenum, and zirconium. The detailed method is presented by Yoshida and Tirumurti [13]. The curve is fairly close to that of pure titanium and represents fairly well the three alloys (within 5%). The Hugoniot curve for the powder was obtained by means of the Mie–Gruneisen equation of state

$$P = P_h + \rho\gamma (E - E_h)$$

where P_h and E_h are the pressure and specific internal energy alloy the solid Hugoniot line; P and E are the pressure and specific internal energy of the porous material; γ the Gruneisen ratio (assumed to be proportional to the specific volume); ρ the density.

The Hugoniot curves for the explosives were traced parallel to the ones for the explosives at ideal detonation, passing through the Chapman–Jouguet points corrected for non-ideality as explained by Meyers and Wang [12].

From these graphical representations of the equations of state for powder, explosives, and iron, the initial pressures can be determined by means of the impedance matching technique. The curve for iron is reversed and intersect the particle velocity axis at the velocity equal to the flyer-tube velocity, calculated from the modified Gurney equation [12]

$$V_p = (2E)^{1/2}\left\{\frac{3}{\left[5\left(\frac{m}{c}\right) + 2\left(\frac{m}{c}\right)^2 \frac{R + r_0}{r_0} + \frac{2r_0}{R + r_0}\right]}\right\}^{1/2}$$

where E is the Gurney energy [14] and m/c is the ratio between the flyer tube mass and explosive mass. R and r_0 are the outer radius of the explosive charge and the outer radius of the flyer tube, respectively. For the explosives used in the present investigation the value of $(2E)^{1/2}$ was assumed to be equal to 1200 m sec^{-1} (for ANFO) and 1370 m sec^{-1} (for TNT). This yields flyer tube velocities of 1620 and 1640 m sec^{-1} using an explosive cylinder with 15.2 cm diameter. In Fig. 3, the reflected iron curve at this velocity intersects the Ti-17 powder curve at a pressure of 12.4 GPa. This is the initial pressure in the powder for the flyer-tube technique. In contrast, the curve for ANFO intersects the powder curve at a pressure of approximately 4.4 GPa. Thus, these preliminary calculations show that the flyer-tube technique generates pressures that are several times higher than the single-tube technique. The nature of the cylindrical geometry is such that the shock-wave amplitude changes as the shock wave propagates into the powder. The calculation of the change in shock-wave profile through the powder requires numerical methods and is presented by Reaugh [15]. One tries to obtain a shock wave that has an amplitude as constant as possible in these systems, to ensure uniform consolidation.

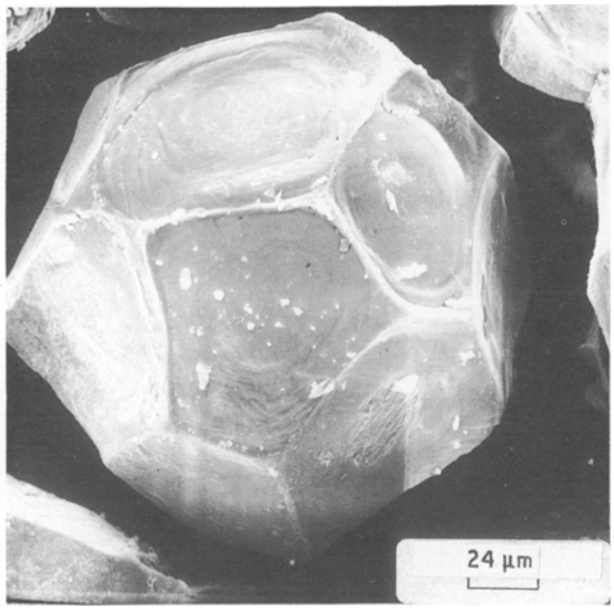

Figure 4 Scanning electron micrograph showing that powder particles underwent a considerable amount of deformation; the particles were initially spherical.

The explosives used were ANFO and TNT and the detonation velocities ranged from 3000 to 3700 m sec^{-1} for ANFO and 3500 to 4500 m sec^{-1} for TNT. Standard metallographic techniques were used for the preparation of specimens for optical and electron microscopy. Tensile tests were conducted at General Electric Aircraft Engine Division at ambient and high temperatures. The speciemens were cylindrical with threaded ends. Their diameter (in the reduced section) was 4 mm, the gauge length was 20 mm and the initial overall length was 50 mm. They were machined so that the specimen axis was parallel to the compacted cylinder axis. The ends were shot-peened

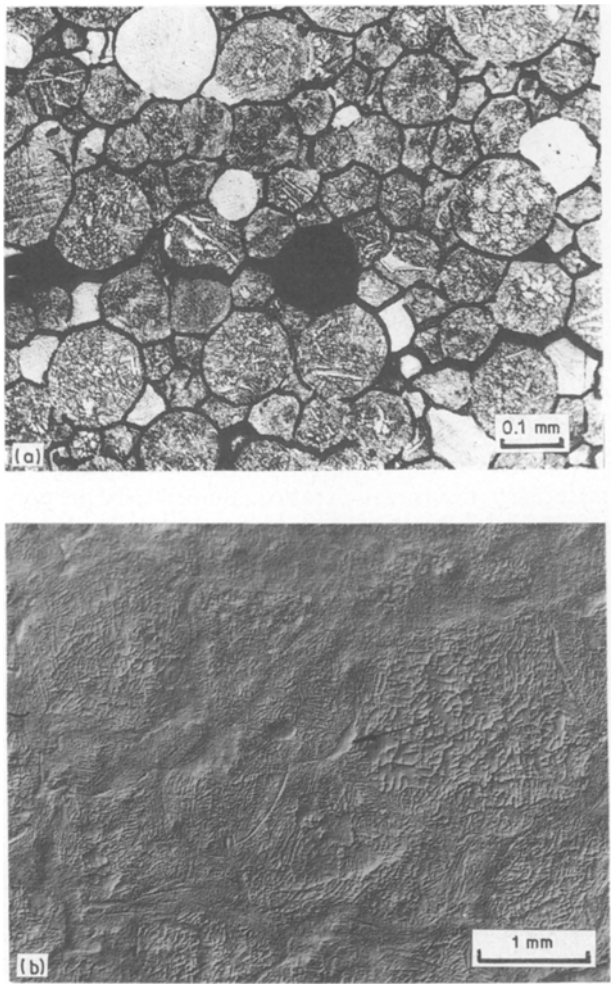

Figure 5 Comparison of structures between compacts of Ti-17 obtained with (a) single-tube and (b) double-tube technique.

Figure 6 Transmission electron micrograph showing planar arrays of dislocations in Ti-17.

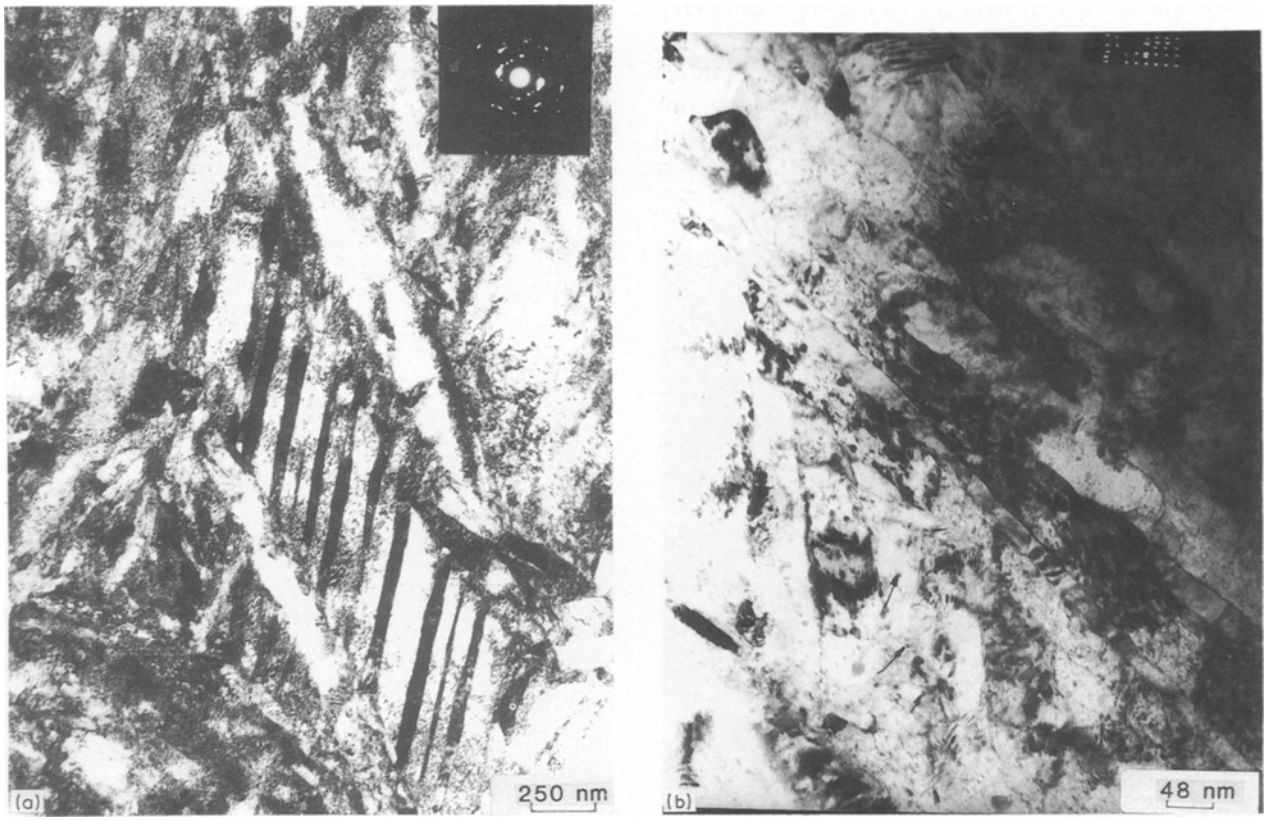

Figure 7 Transmission electron micrograph showing (a) a lath structure with high dislocation and twin densities and (b) fine equiaxed grains and Er_2O_3 dispersoids.

in order to decrease the tendency for fracture initiation in the threads.

3. Results and discussion

3.1. Microstructure

Twenty one consolidation experiments were conducted in this investigation. Generally, the powder particles underwent a considerable amount of deformation. This is illustrated in Fig. 4 that shows a particle that was subjected to shock consolidation without bonding (insufficient pressure for jetting and melting between particles).

Single-tube compaction yielded compacts with considerable density of voids and cracks. The differences are clearly evident in Fig. 5. One of the regions that underwent melting is indicated with an arrow. This improved bonding for the double-tube (or flyer-tube) technique is a direct result of the higher pressure.

Transmission electron microscopy revealed the substructural features of the shock-consolidated and shock-consolidated plus aged alloys. Fig. 6 shows a triple point and dense dislocation arrays in the three grains of Ti-17. These arrays of dislocations in high densities are typical of shocked materials, as described by Meyers and Murr [17]. This region is characteristic of the interiors of the powders.

The titanium alloys strengthened by erbia have been the object of considerable study. The rapid solidification process allows the retention of erbia as very small dispersions; subsequent consolidation at ambient or moderately low temperatures will retain this fine dispersion (that provides good creep resistance). Thus, shock consolidation has been envisaged as a technique to accomplish this goal. Fig. 7 shows transmission electron micrographs of the centre and particle interfaces for shock-consolidated Ti-6242 + Er

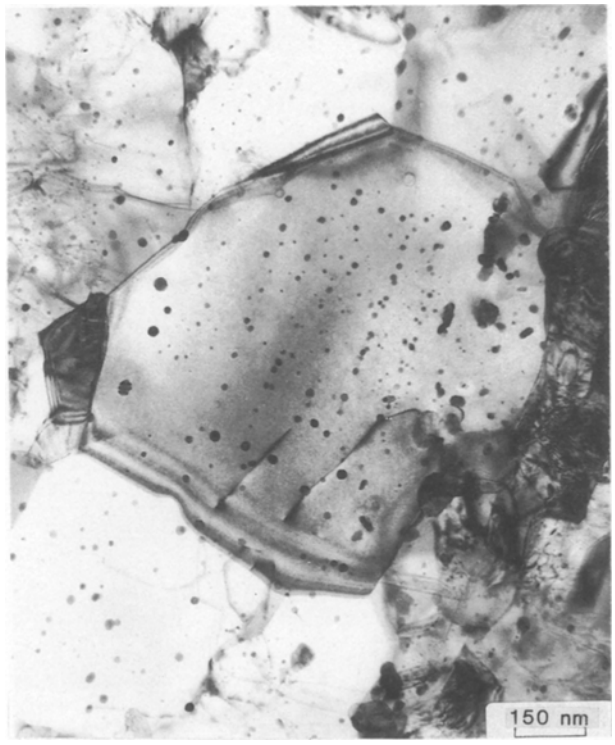

Figure 8 Transmission electron micrograph of shock consolidated Ti-6242 + Er after 2 h annealing at 870 °C.

alloy. The dense lath structure of Fig. 7a is characteristic of the interior of the particles and is due to shock-induced twinning and phase transformations. Twinning is evident from twin spots in the diffraction pattern. The substructure of Fig. 7b is very different. It shows small equiaxed grains with an approximate size

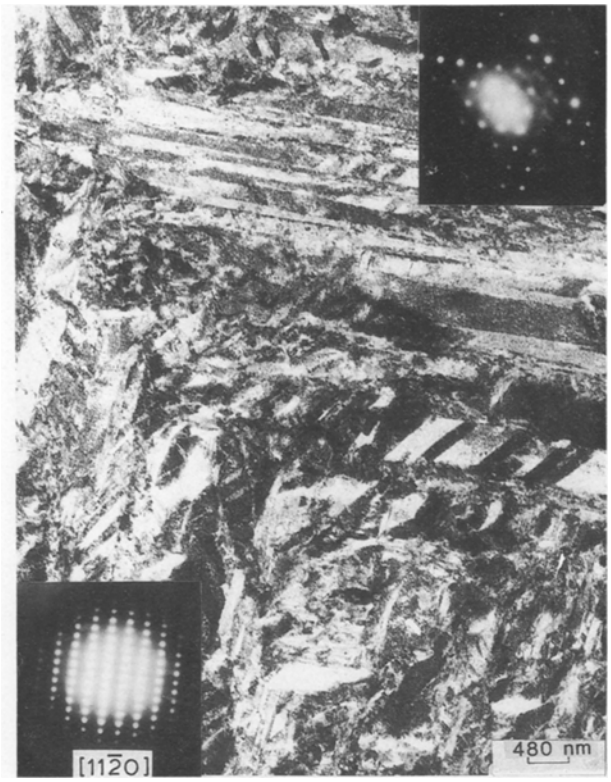

Figure 9 Transmission electron micrograph showing lath structure in Ti-662 compact with [1 1 2 0] alpha diffraction pattern (bottom).

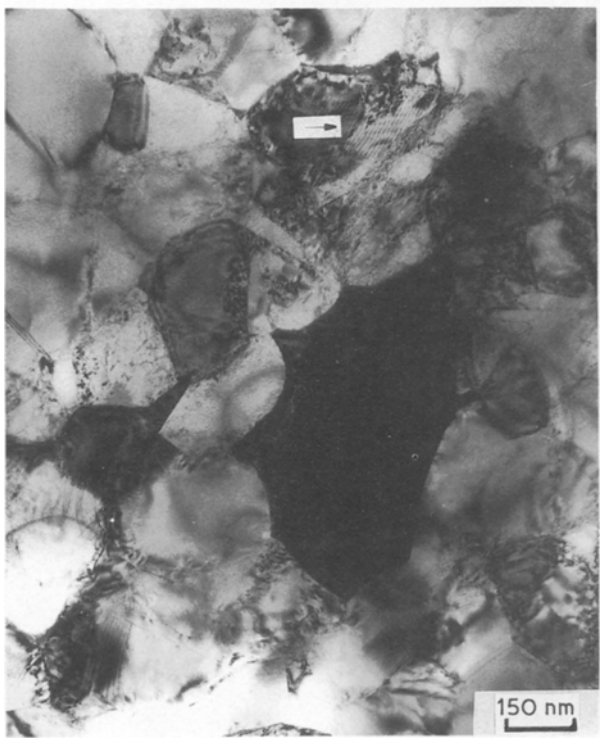

Figure 10 Transmission electron micrograph showing a microcrystalline area.

Figure 11 Transmission electron micrograph showing partial recrystallization (after heat treatment).

Figure 12 Transmission electron micrograph showing interface between particles. Regions marked (a), (b), (c) and (d) shown detail in Fig. 13.

of 0.05 μm. The very low dislocation density means that it is believed that this region underwent either melting or recrystallization. Some Er_2O_3 particles can be seen; they are marked with arrows. In order to

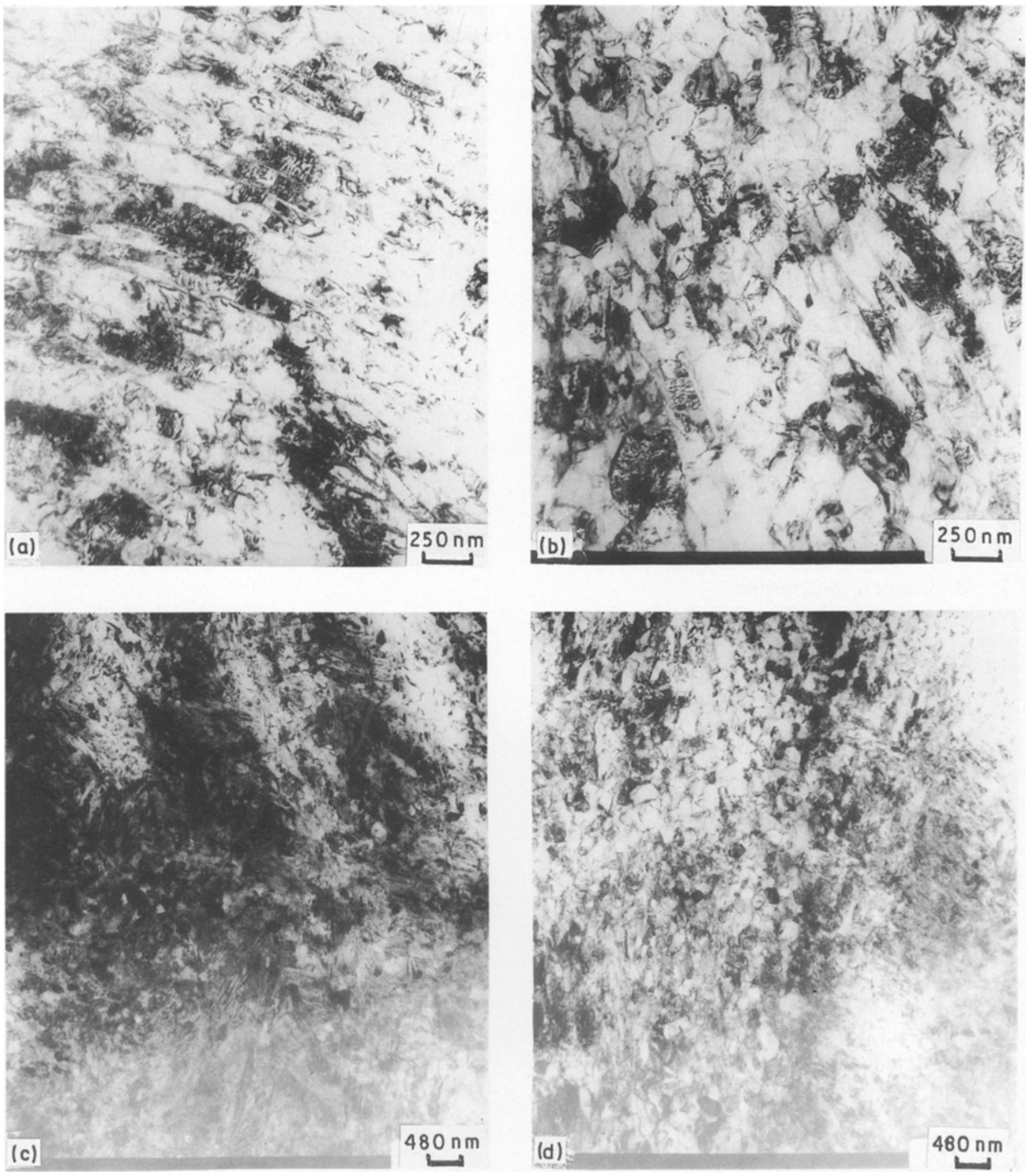

Figure 13 (a) and (b) Regions affected by interparticle heating; (c) region exhibiting laths; (d) boundary between heat-affected and shock hardening region.

reveal the erbia particles more clearly, and to demonstrate that the consolidation process did not significantly increase their size, annealing treatments of shock consolidated alloys were conducted, followed by TEM observations. The substructure after 2 h annealing at 870 °C is shown in Fig. 8. The Er_2O_3 dispersoids are clearly observed. Their size and spacing are such that they are effective high temperature strengtheners. There seems to be a tendency for them to arrange themselves in rows.

Similar dominant types of microstructures (containing laths and equiaxed grains) as seen in Ti-6242 + 1% Er are observed in Ti-662 compacts. Fig. 9 shows the lath structure produced by the rapid solidification process. This martensitic structure is already highly dislocated and shock consolidation does not alter it significantly. The structure shown in Fig. 10 is completely different. It consists of equiaxed grains with approximately 0.2 μm diameter. The dislocation density is relatively low, and this is evidence of either recrystallization or melting and resolidification. The parallel fringes (arrowed) are either from grain-boundary dislocations or a Moiré pattern from two superimposed grains. The darker grain (that diffracts the beam) exhibits a high curvature at the boundaries and the curvature is such that it is growing. The three diffraction patterns taken diagonally along the specimen indicate the misorientation between grains. After

heat treatment, partial recrystallization occurs with the equiaxed grains forming in the lath structure.

Fig. 11 shows a region of Ti-662 after heat treatment; partial recrystallization occurred with the formation of equiaxed grains along channels produced in the lath structure. These two phases were identified; the clear area is the α phase, and the dark area is the transformed β phase.

Fig. 12 shows a micrograph, at lower magnification, that encompasses the region affected by the thermal excursion due to the interaction between adjacent particles. Different regions marked (a), (b), (c), and (d) are identified on it. Higher magnification electron micrographs are shown in Fig. 13a, b, c, and d, respectively. A range of microstructures is visible. Fig. 13a and b show elongated micrograins which seem to have a low dislocation density. Fig. 13d shows the interface between a microcrystalline and a region with high dislocation density, while Fig. 13c shows the lath structure due to shock-wave propagation.

3.2. Mechanical properties

The hardness of the as-received Ti-17 powder increased considerably from 325 HV in the as-received condition to 500 HV in the consolidated condition. Similar results were observed in Ti-662 powder (362 HV to 480 HV) and Ti-6242 + 1% Er powder (from 413 HV to 435 HV). Micro-indentations were made on cross-sections cut toward the top and bottom parts of each compact. The hardnesses were found to be uniform throughout the cross-section. The microhardness of Ti-662 compacts after ageing was also measured and was found to be lower than that of as compacted condition.

Tensile tests carried out on consolidated Ti-17 after ageing heat treatments showed better strength properties when compared with the as-cast material. The average 0.2% yield strength and ultimate tensile strength were 1215 and 1233 MPa, respectively, for the shocked and aged alloy. In contrast, the average yield strength and ultimate strength of the as-cast Ti-17 alloys are generally around 1069 and 1138 MPa, respectively [18]. The ductility of compact was poor compared to the as-cast Ti-17 alloys.

The tensile strengths of the Ti-662 compacts were slightly lower than the standard forged specimen (Fig. 14a). The ductility of the compact in the as-received condition was very poor compared to the standard forged specimen (Fig. 14b). However, after 870 °C and 2 h HIP processing, the ductility at room temperature was better than the standard forged specimen. The increase in ductility with HIP can be attributed to the healing of voids and microcracks. Even a small fraction of voids can have a marked negative effect on elongation.

Some of the fracture surfaces of poorly consolidated specimens (broken easily by hand), and the failed tensile samples were observed with a scanning electron microscope. The fracture surfaces of the sample (broken by hand) showed that the individual particle surfaces were heavily deformed and contained facets (Fig. 15a). No evidence of melting during shock compaction was present in these facets. Particles showed mechanical interlocking with each other. The tyical feature of the surface observed in the well compacted specimens is the dimple structure which is characteristic of the ductile fracture mode, Fig. 16(a). It is thought that the ductile material is formed by interparticle melting–recrystallization. Voids and microcracks were also observed in these ductile regions. Voids are thought to form due to either entrapped air which exists because of absence of vacuum, or due to shrinkage during solidification of the molten material (which is similar to the tearing defects in cast material). These defects are believed to be crack initiation sites. The cracks tend to propagate along the particle boundaries in an interparticle mode.

3.3. Scale-up experiments

Cylinders with 5, 7.5, and 10 cm diameters were successively consolidated by scaling up the consolidation fixture of Fig. 1b while maintaining a constant initial shock pressure. The microstructures of the scaled-up

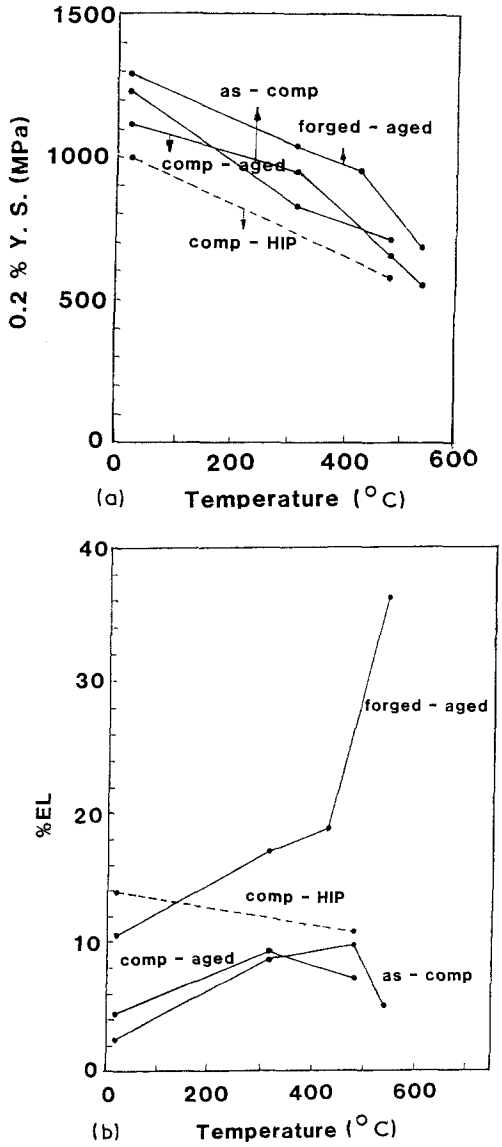

Figure 14 Variation of (a) yield stress and (b) total elongation with temperature for Ti-662 in shock-consolidated, shock-consolidated + aged (570 °C for 4 hr), shock-consolidated + HIPped conditions; forged + aged (570 °C for 4 h) material given as comparison.

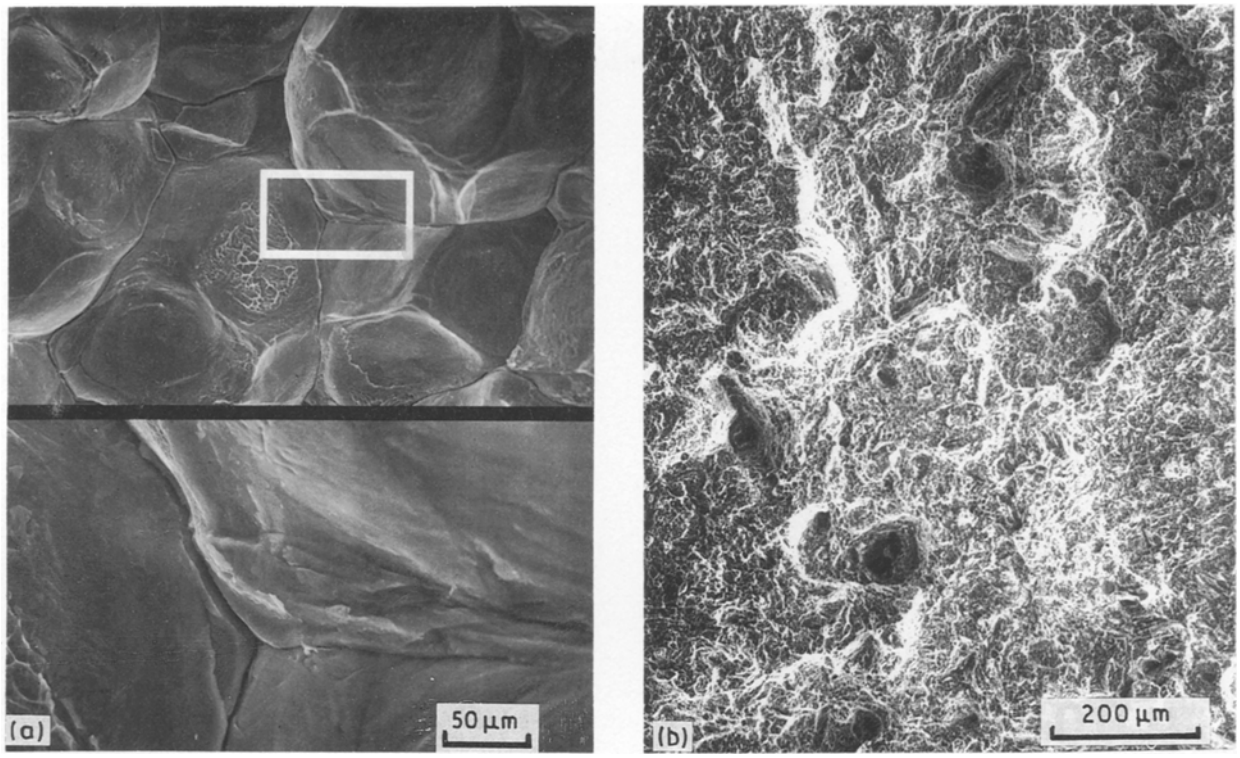

Figure 15 (a) Scanning electron fractograph of poorly shock-consolidated material; notice easy separation at particle interfaces. (b) Scanning electron fractograph of well consolidated material; the dimple morphology is characteristic of the ductile fracture mode (interparticle).

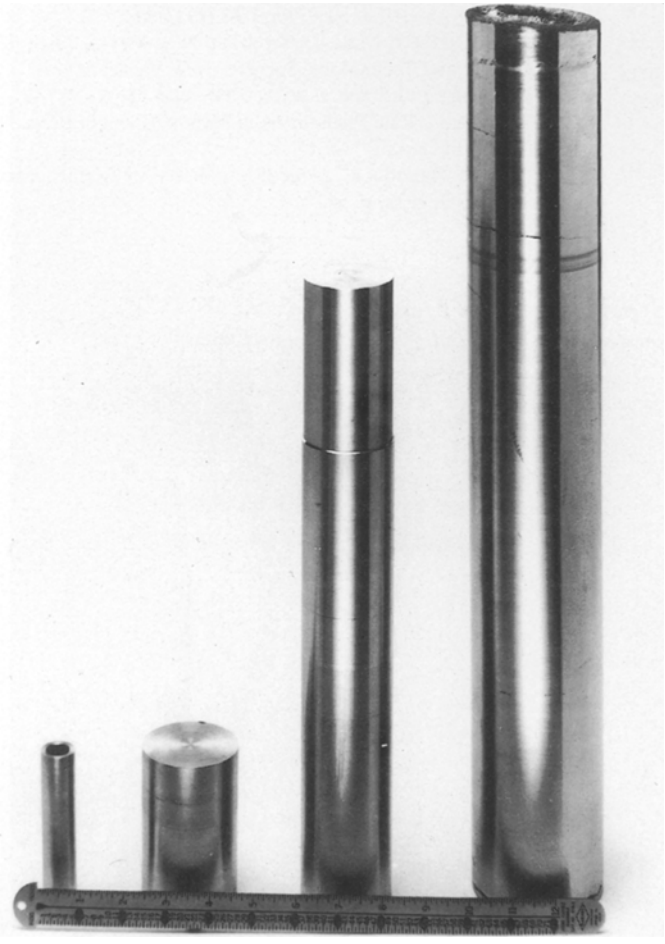

Figure 16 Shock-compacted cylinders of different sizes showing that scalling up in size can be achieved.

compacts were virtually identical to that of the smaller compacts (2.5 cm diameter). The various compact sizes are shown in Fig. 16. The largest compact, in the right-hand side, had a mass of 10 kg.

4. Conclusions

The conclusions are as follows.

(1) Shock consolidation of three rapidly solidified titanium alloy powders – Ti-17, Ti-662, and Ti-6242 + 1% Er – was successfully carried out.

(2) Optical microscopy revealed that the microstructural requirement for good compaction is the formation, during the shock propagation process, of melting pools between the particles.

(3) Observation of the shock-consolidated structures by transmission electron microscopy showed essentially two regions.

(a) a severely shock-affected region characterized by high dislocation density (for Ti-17) and twins and laths (for the other two alloys). This represents the typical structure of the particle interiors.

(b) a region consisting of equiaxed micrograins with low dislocation density in the interiors. This represents the interparticle regions, in which recrystallization and/or melting and rapid resolidification has occurred.

(4) Shock consolidation of the titanium alloy containing erbia did not result in the exaggerated growth of these dispersoids; thus, the high-temperature strengthening phase is retained.

(5) The yield and tensile strengths of shock consolidated and shock consolidated + aged alloys are of the same order as those of forged and cast alloys. The ductility is, however, considerably lower, and it does not show any marked increase at higher temperature. Hipping the shock-consolidated titanium alloy Ti-662 considerably increases the total elongation.

(6) The process of shock consolidation does seem to lend itself to scale-up without difficulty.

Acknowledgements

This research was supported by General Electric Company and by the Center for Explosives Technology Research. Special gratitude is extended to the staff of TERA for performing the shock consolidation experiments and to Mr A. Johnson, Manager of Advanced Metallic Materials, GE, for providing funding for this program.

References

1. R. PRUMMER and G. ZIEGLER, Proceedings 6th International Conference on High Energy Rate Fabrication, 1977, Essen, Germany.
2. V. D. LINSE (ed), "Dynamic Compaction of Metal and Ceramic Powder", National Academy of Sciences, National Materials Advisory Board, NMAB Report 394, 1983, p. 54.
3. M. A. MEYERS, B. B. GUPTA and L. E. MURR, *J. Met.* **33** (1981) 21.
4. R. B. SCHWARZ, R. KASIRAJ, T. VREELAND, Jr. and T. J. AHRENS, *Acta Metall.* **32** (1984) 1243.
5. M. A. MEYERS and H.-R. PAK, *J. Mater. Sci.* **20** (1985) 2133.
6. D. G. MORRIS, *ibid.* **17** (1982) 1789.
7. D. RAYBOULD, *Powder Met.* **25** (1982) 35.
8. W. H. GOURDIN and J. E. SMUGEREVSKY, Proceedings 3rd Conference on Rapid Solidification Processing, edited by R. Mehrabian (National Bureau of Standards, Washington, DC, 1982) p. 565.
9. D. RAYBOULD, in "Shock Waves and High-Strain-Rate Phenomena in Metals", edited by M. A. Meyers and L. E. Murr (Plenum Press, New York, 1981) p. 855.
10. W. H. GOURDIN, *Prog. Mater. Sci.* **30** (1986) 39.
11. R. PRUMMER, in "Explosive Welding, Forming, and Compaction", edited by T. Z. Blazynski (Applied Science, London, 1983) p. 369.
12. M. A. MEYERS and S. H. WANG, *Acta Metall.* **36** (1987) 925.
13. M. YOSHIDA and TIRUMURTI, Center for Explosives Technology Research, 1986, unpublished results.
14. R. K. GURNEY, Ballistic Research Laboratory, BRL Report 405 (1943).
15. J. E. REAUGH, *J. Appl. Phys.* **61** (1987) 962.
16. H.-L. COKER, M.Sc. Dissertation, New Mexico Institute of Mining and Technology, Socorro, New Mexico (1987).
17. M. A. MEYERS and L. E. MURR, (eds) "Shock Waves and High-Strain-Rate Phenomena in Metals" (Plenum Press, New York, 1981).
18. "Metals Handbook" (American Society of Metals, Metals Park, OH, 1972) p. 342.

Received 8 May
and accepted 29 September 1989